

Adaptive Radar Detection in Heterogeneous Clutter-dominated Environments

Angelo Coluccia^a, Danilo Orlando^b, Giuseppe Ricci^{a,*}

^a*Dipartimento di Ingegneria dell'Innovazione, Università del Salento, Via Monteroni, 73100 Lecce, Italy.*

^b*Engineering Faculty of Università degli Studi "Niccolò Cusano", via Don Carlo Gnocchi 3, 00166 Roma, Italy*

Abstract

In this paper, we propose a new solution for the detection problem of a coherent target in heterogeneous environments. Specifically, we first assume that clutter returns from different range bins share the same covariance structure but different power levels. This model meets the experimental evidence related to non-Gaussian and non-homogeneous scenarios. Then, unlike existing solutions that are based upon estimate and plug methods, we propose an approximation of the generalized likelihood ratio test where the maximizers of the likelihoods are obtained through an alternating estimation procedure. Remarkably, we also prove that such estimation procedure leads to an architecture possessing the constant false alarm rate (CFAR) when a specific initialization is used. The performance analysis, carried out on simulated as well as measured data and in comparison with suitable well-known competitors, highlights that the proposed architecture can overcome the CFAR

*Corresponding author

Email addresses: angelo.coluccia@unisalento.it (Angelo Coluccia), daniilo.orlando@unicusano.it (Danilo Orlando), giuseppe.ricci@unisalento.it (Giuseppe Ricci)

competitors and exhibits a limited loss with respect to the other non-CFAR detectors.

Keywords: Adaptive Radar Detection, Cyclic Estimation, Heterogeneous Environment, Generalized Likelihood Ratio Test, Maximum Likelihood Estimation, Radar, Real Data.

1. Introduction

Nowadays, radar systems are ubiquitous in real life with applications ranging from military to civil field [1]. One of the main implications of such a rapid and endless technological development is that the new operating scenarios have become more challenging. Moreover, they require sophisticated signal processing algorithms that were unimaginable a few decades ago due to the limited computational resources provided by the processing units. Such a complexity forces radar engineers to leave aside the classical design assumptions. In fact, focusing on target detection algorithms, even though the most common design assumptions, namely, the Gaussian distribution for the clutter and the homogeneity of data under test and training samples (homogeneous environment) [2, 3, 4, 5, and references therein], allow for a mathematical tractability of the problem, they are not always valid as corroborated by the experimental measurements [6, 7, 8, 9, 10]. For instance, in high-resolution radars, especially at low grazing angles, clutter is generally modeled as a compound-Gaussian process whose complex envelope results from the product of a speckle component (obeying the complex Gaussian distribution) and a texture component (that is a real and nonnegative random process) [11, 12]. When observed on sufficiently short time intervals, the

compound-Gaussian process degenerates into a spherically invariant random process (SIRP) where the texture can be approximated as a deterministic quantity [11, 12]. In this case, each range bin within the radar reference window is characterized by a specific texture value possibly varying over the range. An asymptotically optimum approximation of the generalized likelihood ratio test (GLRT) to detect a coherent signal in the presence of interference¹ modeled in terms of a SIRP has been derived in [13]. Interestingly, such an architecture coincides with the exact GLRT under the so-called partially-homogeneous environment [14], where data under test and training samples (are complex Gaussian distributed and) share the same interference covariance structure but are characterized by their respective interference power levels. This model represents an intermediate design step between the homogeneous and the “fully-heterogeneous” environment [15].

Generally speaking, design assumptions that account for possible inhomogeneities in the reference window are of primary importance in the radar community since training samples may often be contaminated by power variations over range, clutter discretizes, and other outliers. As a consequence, the volume of homogeneous training data does not allow for reliable estimates (sample-starved scenarios). Different solutions to this limitation have been conceived in the open literature. For instance, the well-known knowledge-based paradigm exploits *a priori* information at the design stage to reduce the requirements in terms of secondary data amount. Other widely used techniques consist of the regularization (or shrinkage) of the sample covari-

¹The terms interference and disturbance are used to denote the joint action of clutter and thermal noise.

ance matrix towards a given matrix [16, 17, 18, 19], of clustering training data into homogeneous subsets [20, 21, 22], or of detecting and suppressing the outliers [23, 24, 25].

With the above remarks in mind, in this paper, we attack the detection of a coherent target assuming the fully-heterogeneous scenario, where data vectors obey the complex Gaussian distribution and share the same structure of the interference covariance matrix but different power levels. As stated above, this model meets the experimental evidence related to non-Gaussian, clutter-dominated environments. Unlike [26, 27, 28, 29, 30], where estimate and plug solutions have been conceived and assessed, herein, we devise a suitable approximation of the GLRT. Specifically, such an approximation is dictated by the fact that the straightforward application of the maximum likelihood approach for parameter estimation under each hypothesis leads to intractable mathematics (at least to the best of authors' knowledge). Therefore, we resort to a cyclic optimization procedure that, at each iteration, moves towards a local stationary point of the likelihoods [31]. Remarkably, we prove that the newly proposed architecture can exhibit the constant false alarm rate (CFAR) property with respect to the clutter covariance structure or the power levels or both according to the specific seeds for the alternating procedure.

Finally, the performance assessment is conducted over simulated as well as real recorded data and in comparison with estimate and plug solutions. The latter are grounded on the normalized matched filter (NMF) [13] coupled with the normalized [32], recursive [27], and persymmetric [29] estimates of the clutter covariance matrix.

The remainder of the paper is organized as follows: the next section is devoted to the design of the detector for heterogeneous clutter-dominated environments. Section 3 assesses its performance also in comparison with the aforementioned counterparts. Moreover, it provides two propositions that establish the CFAR behavior of the proposed architecture. Finally, Section 4 contains some concluding remarks and draws future research lines.

1.1. Notation

Vectors and matrices are denoted by boldface lower-case and upper-case letters, respectively. Symbols $\det(\cdot)$, $(\cdot)^T$, $(\cdot)^\dagger$, $(\cdot)^{-1}$, and $(\cdot)^-$ denote the determinant, transpose, conjugate transpose, inverse, and generalized inverse, respectively. As to numerical sets, \mathbb{C} is the set of complex numbers, $\mathbb{C}^{N \times M}$ is the Euclidean space of $(N \times M)$ -dimensional complex matrices, and \mathbb{C}^N is the Euclidean space of N -dimensional complex vectors. We denote by \mathbf{e}_1 the first vector of the canonical basis for \mathbb{C}^N ; $|z|$ and \bar{z} denote the modulus and the complex conjugate of the complex number z , respectively. The identity matrix of size $N \times N$ is indicated by \mathbf{I}_N . The acronym RV means random variable. The acronym PDF stands for probability density function and we write $\mathbf{x} \sim \mathcal{CN}_N(\mathbf{m}, \mathbf{M})$ if \mathbf{x} is a complex normal N -dimensional random vector with mean value \mathbf{m} and positive definite covariance matrix \mathbf{M} .

2. Clutter-dominated Environment: GLRT-based Design

Let us assume a system that collects N (space, time, or space-time) samples from the range cell under test (CUT). The problem of detecting the possible presence of a coherent return in the given CUT can be formulated

as the following hypothesis testing problem:

$$\begin{cases} H_0 : \mathbf{z} \sim \mathcal{CN}_N(\mathbf{0}, \mathbf{R}), \\ \quad \mathbf{z}_k \sim \mathcal{CN}_N(\mathbf{0}, \gamma_k \mathbf{R}), \quad k = 1, \dots, K, \\ H_1 : \mathbf{z} \sim \mathcal{CN}_N(\alpha \mathbf{v}, \mathbf{R}), \\ \quad \mathbf{z}_k \sim \mathcal{CN}_N(\mathbf{0}, \gamma_k \mathbf{R}), \quad k = 1, \dots, K, \end{cases} \quad (1)$$

where $\mathbf{z} \in \mathbb{C}^N$ is the vector of samples from the CUT, $\mathbf{v} \in \mathbb{C}^N$ is the known (space, time, or space-time) steering vector, $\alpha \in \mathbb{C}$ is an unknown parameter accounting for channel propagation, radar cross section of the target, etc., $\mathbf{R} \in \mathbb{C}^{N \times N}$ is an unknown positive definite covariance matrix accounting for the common correlation among samples of the disturbance, the \mathbf{z}_k s are the N -dimensional secondary data vectors, and $\gamma_1, \dots, \gamma_K > 0$ are unknown parameters taking into account the different power levels of secondary data with respect to the CUT (without loss of generality). Finally, we suppose that $K \geq N$.

We want to determine the GLRT for the problem at hand; it is given by

$$\frac{\max_{\alpha, \mathbf{R}, \boldsymbol{\gamma}} f_1(\mathbf{z}, \mathbf{Z}; \alpha, \mathbf{R}, \boldsymbol{\gamma})}{\max_{\mathbf{R}, \boldsymbol{\gamma}} f_0(\mathbf{z}, \mathbf{Z}; \mathbf{R}, \boldsymbol{\gamma})} \underset{H_0}{\overset{H_1}{>}} \eta$$

where $\boldsymbol{\gamma} = [\gamma_1 \cdots \gamma_K]^T$, $\mathbf{Z} = [\mathbf{z}_1 \cdots \mathbf{z}_K]$, and η is the threshold to be set according to the desired probability of false alarm (P_{fa}) while f_1 and f_0 denote the joint PDFs of the CUT and secondary data under H_1 and H_0 , respectively. We have that the PDF is given by

$$\begin{aligned} f_1(\mathbf{z}, \mathbf{Z}; \alpha, \mathbf{R}, \boldsymbol{\gamma}) &= \frac{1}{\pi^{N(K+1)}} \frac{1}{\prod_{k=1}^K \gamma_k^N} \frac{1}{\det^{K+1}(\mathbf{R})} \\ &\times \exp \left\{ - \left((\mathbf{z} - \alpha \mathbf{v})^\dagger \mathbf{R}^{-1} (\mathbf{z} - \alpha \mathbf{v}) + \sum_{k=1}^K \frac{\mathbf{z}_k^\dagger \mathbf{R}^{-1} \mathbf{z}_k}{\gamma_k} \right) \right\} \end{aligned} \quad (2)$$

under H_1 and under H_0 by

$$f_0(\mathbf{z}, \mathbf{Z}; \mathbf{R}, \boldsymbol{\gamma}) = \frac{1}{\pi^{N(K+1)}} \frac{1}{\prod_{k=1}^K \gamma_k^N} \frac{1}{\det^{K+1}(\mathbf{R})} \\ \times \exp \left\{ - \left(\mathbf{z}^\dagger \mathbf{R}^{-1} \mathbf{z} + \sum_{k=1}^K \frac{\mathbf{z}_k^\dagger \mathbf{R}^{-1} \mathbf{z}_k}{\gamma_k} \right) \right\}.$$

The maximizers of the PDFs with respect to \mathbf{R} , given the remaining parameters, are given by

$$\widehat{\mathbf{R}}_1 = \frac{1}{K+1} \left[(\mathbf{z} - \alpha \mathbf{v})(\mathbf{z} - \alpha \mathbf{v})^\dagger + \sum_{k=1}^K \frac{\mathbf{z}_k \mathbf{z}_k^\dagger}{\gamma_k} \right]$$

and

$$\widehat{\mathbf{R}}_0 = \frac{1}{K+1} \left[\mathbf{z} \mathbf{z}^\dagger + \sum_{k=1}^K \frac{\mathbf{z}_k \mathbf{z}_k^\dagger}{\gamma_k} \right]$$

under H_1 and H_0 , respectively. The corresponding partially-compressed likelihoods can be written as

$$l_1(\alpha, \widehat{\mathbf{R}}_1, \boldsymbol{\gamma}; \mathbf{z}, \mathbf{Z}) = \left(\frac{K+1}{e\pi} \right)^{N(K+1)} \frac{1}{\prod_{k=1}^K \gamma_k^N} \\ \times \frac{1}{\det^{K+1} \left[(\mathbf{z} - \alpha \mathbf{v})(\mathbf{z} - \alpha \mathbf{v})^\dagger + \sum_{k=1}^K \frac{\mathbf{z}_k \mathbf{z}_k^\dagger}{\gamma_k} \right]} \quad (3)$$

under H_1 and under H_0 by

$$l_0(\widehat{\mathbf{R}}_0, \boldsymbol{\gamma}; \mathbf{z}, \mathbf{Z}) = \left(\frac{K+1}{e\pi} \right)^{N(K+1)} \frac{1}{\prod_{k=1}^K \gamma_k^N} \\ \times \frac{1}{\det^{K+1} \left[\mathbf{z} \mathbf{z}^\dagger + \sum_{k=1}^K \frac{\mathbf{z}_k \mathbf{z}_k^\dagger}{\gamma_k} \right]}. \quad (4)$$

At authors' knowledge maximization with respect to both α and the γ_k s under H_1 and with respect to the γ_k s under H_0 cannot be conducted in closed form. For this reason, we consider an alternating procedure [31].

More precisely, under H_1 , given the t th estimate of the γ_k s, say $\widehat{\gamma}_k^{1,(t)}$, $k = 1, \dots, K$, we can maximize eq. (3) with respect to α , thus obtaining $\widehat{\alpha}^{(t+1)}$; moreover, given $\widehat{\alpha}^{(t+1)}$ and the $\widehat{\gamma}_k^{1,(t+1)}$ s, $k = 1, \dots, h-1$, together with the $\widehat{\gamma}_k^{1,(t)}$, $k = h+1, \dots, K$, we can maximize eq. (3) with respect to γ_h , thus obtaining $\widehat{\gamma}_h^{1,(t+1)}$. Under H_0 we can proceed in a similar way to maximize eq. (4) with respect to the γ_k s, $k = 1, \dots, K$, assuming that $\alpha = 0$.

In order to maximize eq. (3) with respect to α we minimize the following function

$$f_1(\alpha) = \det \left[(\mathbf{z} - \alpha \mathbf{v})(\mathbf{z} - \alpha \mathbf{v})^\dagger + \mathbf{A}^{(t)} \right]$$

where $\mathbf{A}^{(t)} = \sum_{k=1}^K \frac{\mathbf{z}_k \mathbf{z}_k^\dagger}{\widehat{\gamma}_k^{1,(t)}}$ is a positive definite matrix. It turns out that

$$f_1(\alpha) = \det \left(\mathbf{A}^{(t)} \right) \left[1 + (\mathbf{z} - \alpha \mathbf{v})^\dagger \left(\mathbf{A}^{(t)} \right)^{-1} (\mathbf{z} - \alpha \mathbf{v}) \right]$$

is minimized by

$$\widehat{\alpha}^{(t+1)} = \frac{\mathbf{v}^\dagger \left(\mathbf{A}^{(t)} \right)^{-1} \mathbf{z}}{\mathbf{v}^\dagger \left(\mathbf{A}^{(t)} \right)^{-1} \mathbf{v}}. \quad (5)$$

Let us introduce the function

$$\begin{aligned} f_2(\gamma_h) &= \gamma_h^N \det^{K+1} \left[(\mathbf{z} - \widehat{\alpha}^{(t+1)} \mathbf{v})(\mathbf{z} - \widehat{\alpha}^{(t+1)} \mathbf{v})^\dagger \right. \\ &\quad \left. + \sum_{k=1}^{h-1} \frac{\mathbf{z}_k \mathbf{z}_k^\dagger}{\widehat{\gamma}_k^{1,(t+1)}} + \sum_{k=h+1}^K \frac{\mathbf{z}_k \mathbf{z}_k^\dagger}{\widehat{\gamma}_k^{1,(t)}} + \frac{1}{\gamma_h} \mathbf{z}_h \mathbf{z}_h^\dagger \right] \\ &= \gamma_h^N \det^{K+1} \left[\mathbf{B}_h^{1,(t+1)} + \frac{1}{\gamma_h} \mathbf{z}_h \mathbf{z}_h^\dagger \right] \\ &= \gamma_h^N \det^{K+1} \left(\mathbf{B}_h^{1,(t+1)} \right) \\ &\quad \times \left(1 + \frac{1}{\gamma_h} \mathbf{z}_h^\dagger \left(\mathbf{B}_h^{1,(t+1)} \right)^{-1} \mathbf{z}_h \right)^{K+1} \end{aligned}$$

where

$$\begin{aligned} \mathbf{B}_h^{1,(t+1)} &= (\mathbf{z} - \hat{\alpha}^{(t+1)}\mathbf{v})(\mathbf{z} - \hat{\alpha}^{(t+1)}\mathbf{v})^\dagger + \sum_{k=1}^{h-1} \frac{\mathbf{z}_k \mathbf{z}_k^\dagger}{\hat{\gamma}_k^{1,(t+1)}} \\ &+ \sum_{k=h+1}^K \frac{\mathbf{z}_k \mathbf{z}_k^\dagger}{\hat{\gamma}_k^{1,(t)}} \end{aligned} \quad (6)$$

is a positive definite matrix. Since $\lim_{\gamma_h \rightarrow 0} f_2(\gamma_h) = +\infty$ and $\lim_{\gamma_h \rightarrow +\infty} f_2(\gamma_h) = +\infty$, it follows that the minimum is attained at a stationary point of f_2 .

Moreover, the derivative of f_2 is given by

$$\begin{aligned} \frac{d}{d\gamma_h} f_2(\gamma_h) &= N\gamma_h^{N-1} \det^{K+1}(\mathbf{B}_h^{1,(t+1)}) \left(1 + \frac{1}{\gamma_h} \mathbf{z}_h^\dagger (\mathbf{B}_h^{1,(t+1)})^{-1} \mathbf{z}_h\right)^{K+1} \\ &+ \gamma_h^N \det^{K+1}(\mathbf{B}_h^{1,(t+1)}) (K+1) \left(1 + \frac{1}{\gamma_h} \mathbf{z}_h^\dagger (\mathbf{B}_h^{1,(t+1)})^{-1} \mathbf{z}_h\right)^K \\ &\times \left(-\frac{1}{\gamma_h^2} \mathbf{z}_h^\dagger (\mathbf{B}_h^{1,(t+1)})^{-1} \mathbf{z}_h\right). \end{aligned}$$

Thus, the minimizer is given by

$$\hat{\gamma}_h^{1,(t+1)} = \frac{K+1-N}{N} \mathbf{z}_h^\dagger (\mathbf{B}_h^{1,(t+1)})^{-1} \mathbf{z}_h. \quad (7)$$

Summarizing, to implement the proposed detector, we start with an initial estimate of the γ_k s under H_1 , say $\hat{\gamma}_k^{1,(0)}$ s, and use eqs. (5) and (7) to obtain $\hat{\alpha}^{(1)}$ and $\hat{\gamma}_k^{1,(1)}$, $k = 1, \dots, K$, respectively, and after t_{\max} iterations (see the stopping criterion below) $\hat{\alpha}^{(t_{\max})}$ and $\hat{\gamma}_k^{1,(t_{\max})}$, $k = 1, \dots, K$. Similarly, we compute the estimate of the γ_k s under H_0 , say $\hat{\gamma}_k^{0,(t_{\max})}$, $k = 1, \dots, K$. As a matter of fact, we have to modify eq. (7) by replacing $\mathbf{B}_h^{1,(t+1)}$ of eq. (6) with

$$\mathbf{B}_h^{0,(t+1)} = \mathbf{z}\mathbf{z}^\dagger + \sum_{k=1}^{h-1} \frac{\mathbf{z}_k \mathbf{z}_k^\dagger}{\hat{\gamma}_k^{0,(t+1)}} + \sum_{k=h+1}^K \frac{\mathbf{z}_k \mathbf{z}_k^\dagger}{\hat{\gamma}_k^{0,(t)}}. \quad (8)$$

The entire procedure may terminate after t_{\max} iterations, where t_{\max} is such that

$$\Delta\mathcal{L}(t_{\max}) = \frac{|\mathcal{L}(t_{\max}) - \mathcal{L}(t_{\max} - 1)|}{|\mathcal{L}(t_{\max} - 1)|} < \epsilon, \quad (9)$$

where $\epsilon > 0$ and $\mathcal{L}(t)$ is the log-likelihood function at the t th iteration, or t_{\max} is the maximum allowable number of iterations set according to the selected compromise between performance and computational requirements.

Finally, we obtain the following approximation of the GLRT statistic

$$\frac{\left[\frac{\prod_{k=1}^K \hat{\gamma}_k^{0,(t_{\max})}}{\prod_{k=1}^K \hat{\gamma}_k^{1,(t_{\max})}} \right]^{\frac{N}{K+1}} \det \left[\mathbf{z}\mathbf{z}^\dagger + \sum_{k=1}^K \frac{\mathbf{z}_k \mathbf{z}_k^\dagger}{\hat{\gamma}_k^{0,(t_{\max})}} \right]}{\det \left[(\mathbf{z} - \hat{\alpha}^{(t_{\max})} \mathbf{v})(\mathbf{z} - \hat{\alpha}^{(t_{\max})} \mathbf{v})^\dagger + \sum_{k=1}^K \frac{\mathbf{z}_k \mathbf{z}_k^\dagger}{\hat{\gamma}_k^{1,(t_{\max})}} \right]}. \quad (10)$$

3. Performance assessment

This section is devoted to the analysis of the proposed detector and consists of two subsections. The first subsection proves that the proposed detector can be CFAR with respect to both the matrix \mathbf{R} and the parameters $\gamma_1, \dots, \gamma_K$ under the design assumptions. The aim of the latter subsection is twofold. Firstly, it assesses the performance of the detector in comparison to natural competitors and also in the presence of possible mismatches between the nominal and the actual operating conditions by resorting to Monte Carlo simulation. In particular, we investigate the effects due to the presence of a small, but non-negligible, thermal noise component (actually we will assume non-Gaussian, clutter-dominated environments). Finally, this subsection contains also illustrative examples obtained using real recorded data.

3.1. Theoretical analysis: CFAR property

In the following we will prove that the proposed detector can possess the CFAR property with respect to \mathbf{R} and the γ_k s under the design assumptions. We start with the following preliminary result.

Lemma 1. *Suppose that the joint distribution of the entries of the random vectors $\widehat{\boldsymbol{\gamma}}^{1,(t)} = [\widehat{\gamma}_1^{1,(t)}, \dots, \widehat{\gamma}_K^{1,(t)}]^T$, $\widehat{\boldsymbol{\gamma}}^{0,(t)} = [\widehat{\gamma}_1^{0,(t)}, \dots, \widehat{\gamma}_K^{0,(t)}]^T$ and $\mathbf{UR}^{-1/2}[\mathbf{z} \mathbf{Z}]$, with \mathbf{U} a unitary matrix such that $\mathbf{UR}^{-1/2}\mathbf{v}$ is aligned with \mathbf{e}_1 (the first vector of the canonical basis), is independent of \mathbf{R} under H_0 . Then, the joint distribution of the entries of the random vectors $\widehat{\boldsymbol{\gamma}}^{1,(t+1)}$, $\widehat{\boldsymbol{\gamma}}^{1,(t)}$, $\widehat{\boldsymbol{\gamma}}^{0,(t+1)}$, $\widehat{\boldsymbol{\gamma}}^{0,(t)}$, $\mathbf{UR}^{-1/2}[\mathbf{z} \mathbf{Z}]$ is also independent of \mathbf{R} under H_0 .*

Proof. See Appendix A. □

We are now in the condition to prove the CFAR property of the proposed detector with respect to \mathbf{R} . In fact, the following theorem holds true.

Theorem 1. *Suppose that the joint distribution of the RVs $\widehat{\gamma}_k^{1,(0)}$, $\widehat{\gamma}_k^{0,(0)}$, $k = 1, \dots, K$, and the entries of $\mathbf{UR}^{-1/2}[\mathbf{z} \mathbf{Z}]$, is independent of \mathbf{R} under H_0 (see Lemma 1 for the definition of \mathbf{U}). Then, the distribution of the statistic (10) is independent of \mathbf{R} under the H_0 hypothesis (and provided that the design assumptions are satisfied).*

Proof. See Appendix A. □

Another preliminary result is

Lemma 2. *Suppose that, under H_0 , $\widehat{\gamma}_k^{1,(t)} = \gamma_k g_k^{1,(t)}(\mathbf{z}, \mathbf{G})$ and $\widehat{\gamma}_k^{0,(t)} = \gamma_k g_k^{0,(t)}(\mathbf{z}, \mathbf{G})$, $k = 1, \dots, K$, with $\mathbf{G} = [\mathbf{z}_1/\sqrt{\gamma_1} \cdots \mathbf{z}_K/\sqrt{\gamma_K}]$. It turns out*

that $\widehat{\gamma}_k^{1,(t+1)} = \gamma_k g_k^{1,(t+1)}(\mathbf{z}, \mathbf{G})$, $\widehat{\gamma}_k^{0,(t+1)} = \gamma_k g_k^{0,(t+1)}(\mathbf{z}, \mathbf{G})$, $k = 1, \dots, K$, and, in addition, $\widehat{\alpha}^{(t+1)} = h^{(t+1)}(\mathbf{z}, \mathbf{G})$ is independent of $\gamma_1, \dots, \gamma_K$.

Proof. See Appendix A. □

Now, we can prove the CFAR property with respect to the scale factors through the following theorem.

Theorem 2. *Suppose that, under H_0 , $\widehat{\gamma}_k^{1,(0)}$ and $\widehat{\gamma}_k^{0,(0)}$, $k = 1, \dots, K$, satisfy the assumptions of Lemma 2 for $\widehat{\gamma}_k^{1,(t)}$ and $\widehat{\gamma}_k^{0,(t)}$, $k = 1, \dots, K$. Then the decision statistic (10) possesses the CFAR property with respect to the γ_k s.*

Proof. See Appendix A. □

As final remark of this subsection, we give an example of initialization of the γ_k s that satisfies the assumptions of Theorem 1 and 2 and, hence, guarantees the CFAR property of the proposed detector. The initialization is

$$\widehat{\gamma}_k^{i,(0)} = \mathbf{z}_k^\dagger (\mathbf{z} \mathbf{z}^\dagger)^- \mathbf{z}_k, \quad k = 1, \dots, K, \quad i = 0, 1,$$

where we recall that $(\cdot)^-$ denotes a generalized inverse of the matrix argument. As a matter of fact, it is straightforward to check that the assumptions of Theorem 2 are satisfied. Moreover, we have that

$$\begin{aligned} \mathbf{z}_k^\dagger (\mathbf{z} \mathbf{z}^\dagger)^- \mathbf{z}_k &= \left(\mathbf{U} \mathbf{R}^{-1/2} \mathbf{z}_k \right)^\dagger \mathbf{U} \mathbf{R}^{1/2} (\mathbf{z} \mathbf{z}^\dagger)^- \mathbf{R}^{1/2} \mathbf{U}^\dagger \mathbf{U} \mathbf{R}^{-1/2} \mathbf{z}_k \\ &= \left(\mathbf{U} \mathbf{R}^{-1/2} \mathbf{z}_k \right)^\dagger \left(\mathbf{U} \mathbf{R}^{-1/2} (\mathbf{z} \mathbf{z}^\dagger) \mathbf{R}^{-1/2} \mathbf{U}^\dagger \right)^- \mathbf{U} \mathbf{R}^{-1/2} \mathbf{z}_k \\ &= \left(\mathbf{U} \mathbf{R}^{-1/2} \mathbf{z}_k \right)^\dagger \left(\mathbf{U} \mathbf{R}^{-1/2} \mathbf{z} \left(\mathbf{U} \mathbf{R}^{-1/2} \mathbf{z} \right)^\dagger \right)^- \mathbf{U} \mathbf{R}^{-1/2} \mathbf{z}_k \end{aligned}$$

where we have used property (9) in 3.6.1 of [33]. Thus, also the assumptions of Theorem 1 are satisfied.

3.2. Detection performance: simulated and real recorded data

In what follows, we analyze the performance of the proposed detector against natural competitors. In particular, we consider the NMF detector [13], coupled with three different estimates of the disturbance covariance matrix:

- the so-called normalized sample covariance matrix defined in [32];
- the estimate relying on the recursive procedure devised in [27];
- the recursive estimate exploiting the persymmetric structure of the covariance matrix proposed in [29].

The considered competitors are reference benchmarks for detection in heterogeneous scenarios. The number of iterations for the above recursive estimators is set to three, since this number is sufficient to guarantee an acceptable convergence as corroborated by the related literature.

Starting the analysis from the simulated data, a desired $P_{fa} = 10^{-3}$ is assumed and the performance is assessed by Monte Carlo simulation with $100/P_{fa}$ independent trials to set the thresholds as well as to estimate the P_{fa} ; the P_d values are estimated based upon 10^3 trials. Moreover, we set $N = 8$, $K = 16$, and use a temporal steering vector with zero Doppler. The non-homogeneous disturbance is then generated according to the compound-Gaussian model, with the texture distributed as the square root of a Gamma random variable with parameters $(\nu, 1/\nu)$ (so that the mean square value is unitary) and the complex normal speckle with exponentially-shaped covariance matrix, i.e., the (m_1, m_2) th entry of the matrix \mathbf{R} is given by $\rho^{|m_1 - m_2|}$,

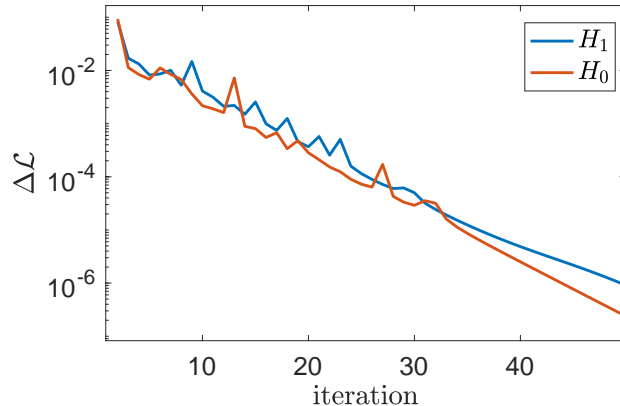


Figure 1: Average log-likelihood relative variation between consecutive iterations for the proposed detector (both hypotheses).

$\rho = 0.95$. Additional white (thermal) noise is also considered in some numerical examples. Specifically, as first step, we show the performance results under the design assumptions, i.e., without thermal noise, then we assess the performance under mismatched conditions, that is considering the presence of both clutter and thermal noise. To this end, we adopt the following general definition for the signal-to-noise ratio (SNR)

$$\text{SNR} = |\alpha|^2 \mathbf{v}^\dagger (\mathbf{R} + \sigma^2 \mathbf{I}_N)^{-1} \mathbf{v}, \quad (11)$$

where $\sigma^2 > 0$ is the thermal noise power and can be set to zero when the proposed detector is assessed under the design assumption.

The number of iterations for the proposed algorithm is set to 20. This value is justified by Fig. 1 where we plot the averaged (over 10^5 Monte Carlo trials) log-likelihood relative variation under both hypotheses as a function of the number of iterations. It turns out that such a variation quickly decreases with the iteration number and is no greater than 10^{-3} after 20 iterations.

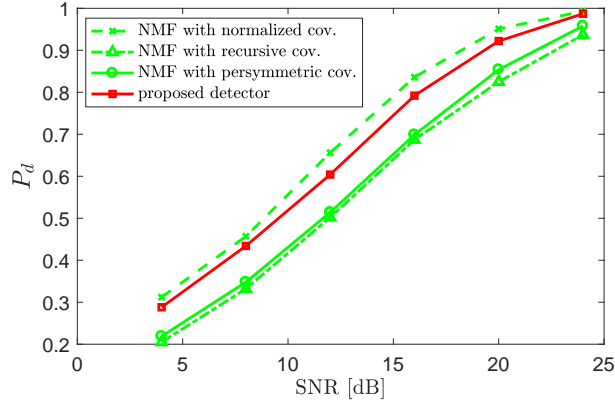


Figure 2: P_d vs SNR of the proposed detector, in comparison with natural competitors, in the clutter-only case.

Fig. 2 reports the curves of P_d versus SNR under the design assumptions (i.e., assuming $\sigma^2 = 0$) and setting $\nu = 0.5$ (this value is also used in Fig. 5). The curves show that the proposed architecture achieves better performance than the considered competitors except for the NMF coupled with the normalized sample covariance matrix. However, the advantage of the latter is basically a consequence of its sensitivity to mismatches of the clutter distribution, i.e., it lacks the CFAR property. This fact is confirmed by Fig. 3 that contains the P_{fa} curves for the considered decision schemes as functions of the actual one-lag correlation coefficient. It is clearly visible that only the NMF with normalized sample covariance matrix is sensitive to mismatches with respect to ρ . In particular, the corresponding P_{fa} values become unacceptably higher in the upper range, whereas the other detectors are theoretically CFAR with respect to ρ in the absence of thermal noise. From the analysis in Sec. 3.1, we also know that all the detectors are CFAR with respect to ν , and this is confirmed in the numerical results shown in

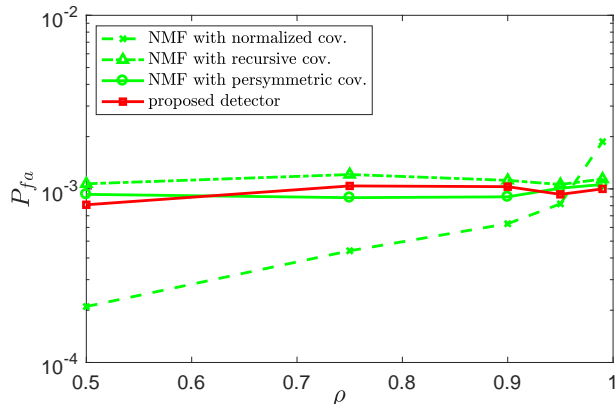


Figure 3: Sensitivity analysis of P_{fa} with respect to mismatched one-lag correlation coefficient of the clutter covariance matrix (nominal value $\rho = 0.95$), in the clutter-only case.

Fig. 4 (again computed over 10^5 Monte Carlo trials).

We now consider the analysis in the presence of thermal noise (i.e., $\sigma^2 > 0$) deviating from the design assumptions. The clutter-to-noise ratio is 40 dB and we consider $\nu = 0.5$. Fig. 5 shows that the proposed decision rule still overcomes the other CFAR competitors in the whole range of SNR. As for the NMF coupled with the normalized sample covariance matrix, it is slightly superior to the proposed detector, but its P_{fa} is more sensitive to clutter parameter variations as shown in Figs. 6 and 7. Indeed, Fig. 6 shows that, while the presence of thermal noise hampers strict CFARness for all detectors, only the NMF with normalized covariance matrix experiences a nonnegligible sensitivity to mismatches on ρ . In Fig. 7, we show the curves of P_{fa} as a function of the actual texture parameter. The results indicate that CFAR detectors share almost the same weak sensitivity with respect to ν but for the NMF coupled with the normalized covariance matrix, which

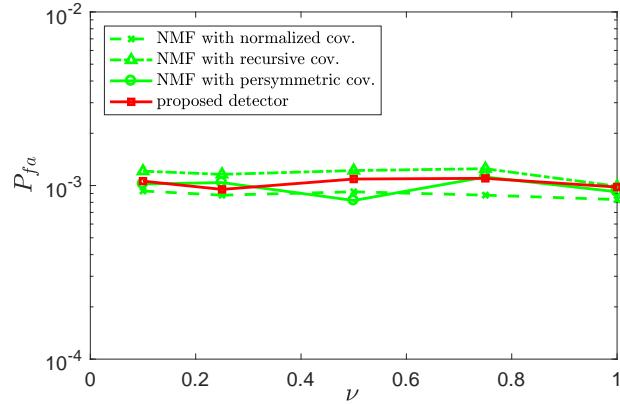


Figure 4: Sensitivity analysis of P_{fa} with respect to mismatched texture parameter of the clutter (nominal value $\nu = 0.5$), in the clutter-only case.

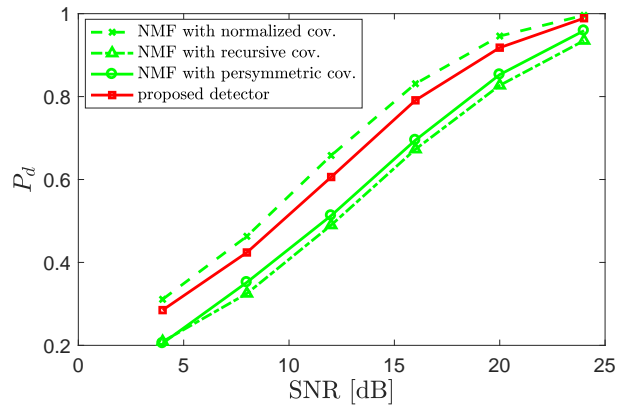


Figure 5: P_d vs SNR of the proposed detector, in comparison with natural competitors, in the clutter plus thermal noise case.

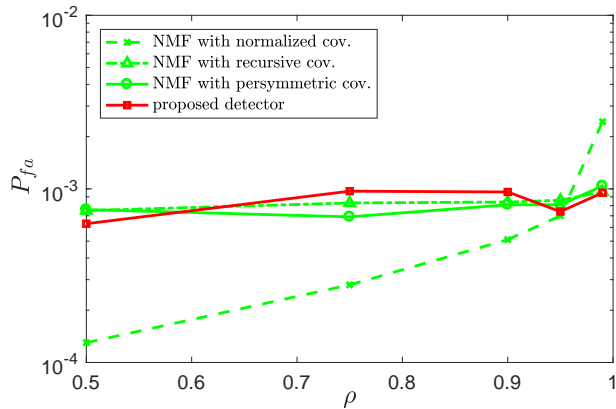


Figure 6: Sensitivity analysis of P_{fa} with respect to mismatched one-lag correlation coefficient of the clutter covariance matrix (nominal value $\rho = 0.95$), in the clutter plus thermal noise case.

experiences a more marked increase in P_{fa} for small values of ν .

In the second and final part of this subsection, we assess the performance of the considered architectures using real L-band land clutter data, recorded in 1985 using the MIT Lincoln Laboratory Phase One radar at the Katahdin Hill site, MIT Lincoln Laboratory. We consider the dataset contained in the file “H067038.3”, which is composed of 30720 temporal returns from 76 range cells with HH polarization. More details can be found in [34, 35] and references therein. Fig. 8 reports the P_d for range bin 30, as function of the SNR defined by² (11). The threshold is set by considering 8-dimensional temporal vectors with 5 pulses of overlap, so as to obtain a sufficient number of snapshots to match the $100/P_{fa}$ rule, for $P_{fa} = 10^{-2}$. Thus, the detectors

²Notice that the covariance matrix used in the SNR definition might be different from the actual covariance matrix.

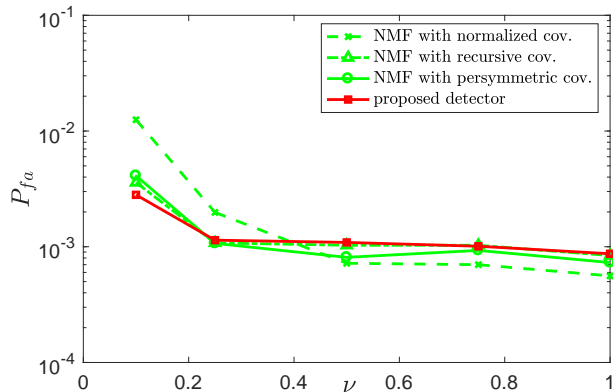


Figure 7: Sensitivity analysis of P_{fa} with respect to mismatched texture parameter of the clutter (nominal value $\nu = 0.5$), in the clutter plus thermal noise case.

work at the same P_{fa} . The target is then added synthetically as done for the simulated data. It turns out that the proposed architecture confirms its excellent behavior with detection performance very close to that of NMF coupled with normalized covariance matrix, which however is not CFAR. Indeed, in order to investigate the CFAR behavior of the considered detectors, in Fig. 9, we report the estimates of the P_{fa} on different range bins, using the same values of the threshold obtained for range bin 30. The proposed detector mostly guarantees P_{fa} values lower than or equal to the nominal P_{fa} , whereas the NMF coupled with the normalized covariance matrix exhibits more significant deviations towards larger values of P_{fa} .

We conclude the performance analysis by showing in Figs. 10 and 11 the results on the Phase One data when the threshold is synthetically set on white noise, i.e., $\mathbf{R} = \mathbf{I}_N$ and $\sigma^2 = 0$, while P_d and P_{fa} are evaluated on real data. Results confirm the goodness of the proposed approach.

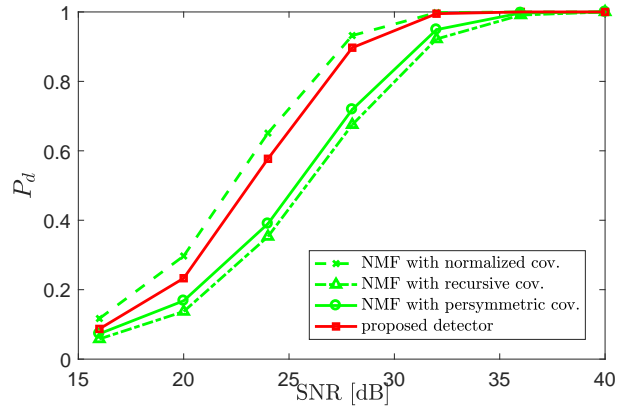


Figure 8: P_d vs SNR of the proposed detector, in comparison with natural competitors, on the Phase One real dataset (range bin 30 for both threshold setting and P_d evaluation).

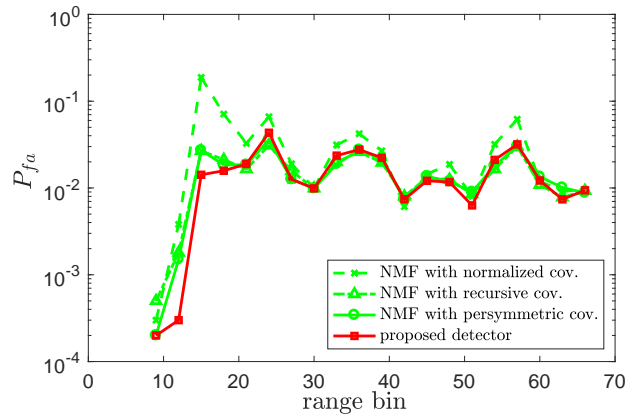


Figure 9: P_{fa} sensitivity for the different range bins, with threshold computed on range bin 30, on the Phase One real dataset.

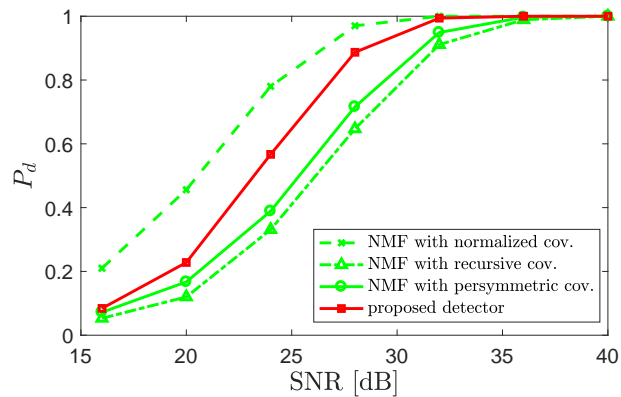


Figure 10: P_d vs SNR of the proposed detector, in comparison with natural competitors, on the Phase One real dataset (white noise for threshold setting and range bin 30 for P_d evaluation).

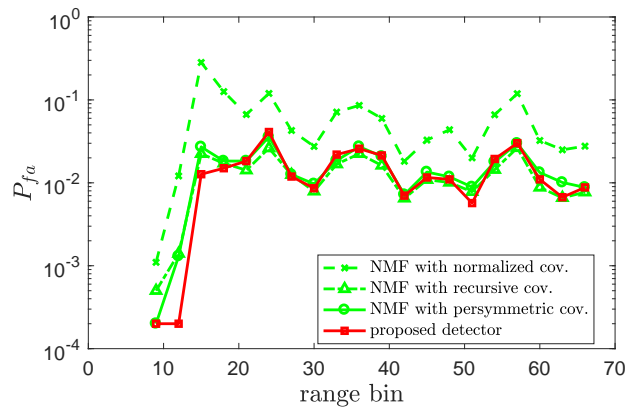


Figure 11: P_{fa} sensitivity for the different range bins, with threshold computed on range bin 30, on the Phase One real dataset (white noise for threshold setting).

4. Conclusion

We have derived an approximation to the GLRT to detect a coherent target in heterogeneous environments. The considered scenario includes clutter returns from different range bins that share the same covariance structure but different power levels as experimentally measured in real environments where the Gaussian assumption is no longer valid. To solve this problem, we have conceived an alternating estimation procedure allowing for an approximation of the GLRT unlike existing solutions that are based upon estimate and plug methods. At the analysis stage, we have performed a theoretical and experimental investigation using both synthetic and real data. Remarkably, we have proved that the proposed estimation procedure leads to an architecture possessing the CFAR property when a specific initialization is used. The illustrative examples have shown that the proposed solution represents an excellent compromise between detection performance and CFAR behavior. As a matter of fact, it provides better detection performance than the CFAR competitors and exhibits a limited loss with respect to the non CFAR detector obtained by coupling the NMF with the normalized sample covariance matrix. Finally, the design of architectures accounting for the different components of the interference covariance matrix is currently under investigation and represents a promising new research line.

Appendix A

Proof of Lemma 1

First observe that $\widehat{\alpha}^{(t+1)}$ can be rewritten as

$$\widehat{\alpha}^{(t+1)} = \frac{\mathbf{u}^\dagger \left(\mathcal{A}^{(t)} \right)^{-1} \boldsymbol{\zeta}}{\mathbf{u}^\dagger \left(\mathcal{A}^{(t)} \right)^{-1} \mathbf{u}} \quad (\text{A.12})$$

where $\boldsymbol{\zeta} = \mathbf{R}^{-1/2} \mathbf{z}$, $\mathbf{u} = \mathbf{R}^{-1/2} \mathbf{v}$, and $\mathcal{A}^{(t)} = \sum_{k=1}^K \frac{\boldsymbol{\zeta}_k \boldsymbol{\zeta}_k^\dagger}{\widehat{\gamma}_k^{1,(t)}}$ with $\boldsymbol{\zeta}_k = \mathbf{R}^{-1/2} \mathbf{z}_k$. Notice that $\boldsymbol{\zeta}$ and the $\boldsymbol{\zeta}_k$ s are independent random vectors with a Gaussian distribution that is independent of \mathbf{R} under H_0 . Moreover, we can rotate \mathbf{u} in order to obtain a vector with a nonzero first entry and the remaining entries equal to zero, i.e., $\mathbf{U}\mathbf{u} = [u \ 0 \ \cdots \ 0]^T$ by using a proper unitary matrix \mathbf{U} that does not modify the statistical characterization of $\boldsymbol{\zeta}$ and the $\boldsymbol{\zeta}_k$ s. Thus, we can also write

$$\widehat{\alpha}^{(t+1)} = \frac{\bar{u} (\mathbf{c}^{(t)})^\dagger \mathbf{U} \boldsymbol{\zeta}}{|u|^2 (\mathbf{c}^{(t)})^\dagger \mathbf{e}_1} \quad (\text{A.13})$$

with $(\mathbf{c}^{(t)})^\dagger$ the first row of the inverse of the matrix $\mathbf{U}\mathcal{A}^{(t)}\mathbf{U}^\dagger$ (recall that \mathbf{e}_1 is the first vector of the canonical basis for $\mathbb{C}^{N \times 1}$). Moreover, $\widehat{\gamma}_1^{1,(t+1)}$, given by eq. (7), can be rewritten as

$$\widehat{\gamma}_1^{1,(t+1)} = \frac{K+1-N}{N} \boldsymbol{\zeta}_1^\dagger \left(\mathcal{B}_1^{1,(t+1)} \right)^{-1} \boldsymbol{\zeta}_1,$$

with

$$\mathcal{B}_1^{1,(t+1)} = (\boldsymbol{\zeta} - \widehat{\alpha}^{(t+1)} \mathbf{u}) (\boldsymbol{\zeta} - \widehat{\alpha}^{(t+1)} \mathbf{u})^\dagger + \sum_{k=2}^K \frac{\boldsymbol{\zeta}_k \boldsymbol{\zeta}_k^\dagger}{\widehat{\gamma}_k^{1,(t)}},$$

and also as

$$\widehat{\gamma}_1^{1,(t+1)} = \frac{K+1-N}{N} (\mathbf{U}\boldsymbol{\zeta}_1)^\dagger \left(\mathbf{U}\mathcal{B}_1^{1,(t+1)}\mathbf{U}^\dagger \right)^{-1} \mathbf{U}\boldsymbol{\zeta}_1 \quad (\text{A.14})$$

with

$$\begin{aligned} \mathbf{U}\mathcal{B}_1^{1,(t+1)}\mathbf{U}^\dagger &= \left(\mathbf{U}\boldsymbol{\zeta} - \frac{(\mathbf{c}^{(t)})^\dagger \mathbf{U}\boldsymbol{\zeta}}{(\mathbf{c}^{(t)})^\dagger \mathbf{e}_1} \mathbf{e}_1 \right) \left(\mathbf{U}\boldsymbol{\zeta} - \frac{(\mathbf{c}^{(t)})^\dagger \mathbf{U}\boldsymbol{\zeta}}{(\mathbf{c}^{(t)})^\dagger \mathbf{e}_1} \mathbf{e}_1 \right)^\dagger \\ &\quad + \sum_{k=2}^K \frac{\mathbf{U}\boldsymbol{\zeta}_k (\mathbf{U}\boldsymbol{\zeta}_k)^\dagger}{\widehat{\gamma}_k^{1,(t)}} \end{aligned}$$

where we have used eq. (A.13). It is apparent that, since the joint distribution of $\widehat{\gamma}_1^{1,(t)}, \dots, \widehat{\gamma}_K^{1,(t)}$ and the entries of $\mathbf{U}\mathbf{R}^{-1/2}[\mathbf{z} \ \mathbf{Z}]$ is independent of \mathbf{R} under H_0 , also the joint distribution of $\widehat{\gamma}_1^{1,(t+1)}, \widehat{\gamma}_1^{1,(t)}, \dots, \widehat{\gamma}_K^{1,(t)}$ and the entries of $\mathbf{U}\mathbf{R}^{-1/2}[\mathbf{z} \ \mathbf{Z}]$ is independent of \mathbf{R} under H_0 . Similarly, $\widehat{\gamma}_2^{1,(t+1)}$, given by eq. (7), can be rewritten as

$$\widehat{\gamma}_2^{1,(t+1)} = \frac{K+1-N}{N} \boldsymbol{\zeta}_2^\dagger \left(\mathcal{B}_2^{1,(t+1)} \right)^{-1} \boldsymbol{\zeta}_2,$$

with

$$\mathcal{B}_2^{1,(t+1)} = (\boldsymbol{\zeta} - \widehat{\alpha}^{(t+1)}\mathbf{u}) (\boldsymbol{\zeta} - \widehat{\alpha}^{(t+1)}\mathbf{u})^\dagger + \frac{\boldsymbol{\zeta}_1 \boldsymbol{\zeta}_1^\dagger}{\widehat{\gamma}_1^{1,(t+1)}} + \sum_{k=3}^K \frac{\boldsymbol{\zeta}_k \boldsymbol{\zeta}_k^\dagger}{\widehat{\gamma}_k^{1,(t)}},$$

and also as

$$\widehat{\gamma}_2^{1,(t+1)} = \frac{K+1-N}{N} (\mathbf{U}\boldsymbol{\zeta}_2)^\dagger \left(\mathbf{U}\mathcal{B}_2^{1,(t+1)}\mathbf{U}^\dagger \right)^{-1} \mathbf{U}\boldsymbol{\zeta}_2$$

with

$$\begin{aligned} \mathbf{U}\mathcal{B}_2^{1,(t+1)}\mathbf{U}^\dagger &= \left(\mathbf{U}\boldsymbol{\zeta} - \frac{(\mathbf{c}^{(t)})^\dagger \mathbf{U}\boldsymbol{\zeta}}{(\mathbf{c}^{(t)})^\dagger \mathbf{e}_1} \mathbf{e}_1 \right) \left(\mathbf{U}\boldsymbol{\zeta} - \frac{(\mathbf{c}^{(t)})^\dagger \mathbf{U}\boldsymbol{\zeta}}{(\mathbf{c}^{(t)})^\dagger \mathbf{e}_1} \mathbf{e}_1 \right)^\dagger \\ &\quad + \frac{\mathbf{U}\boldsymbol{\zeta}_1 (\mathbf{U}\boldsymbol{\zeta}_1)^\dagger}{\widehat{\gamma}_1^{1,(t+1)}} + \sum_{k=3}^K \frac{\mathbf{U}\boldsymbol{\zeta}_k (\mathbf{U}\boldsymbol{\zeta}_k)^\dagger}{\widehat{\gamma}_k^{1,(t)}}. \end{aligned}$$

Thus, the joint distribution of $\widehat{\gamma}_1^{1,(t+1)}, \widehat{\gamma}_2^{1,(t+1)}, \widehat{\gamma}_1^{1,(t)}, \dots, \widehat{\gamma}_K^{1,(t)}$ and the entries of $\mathbf{UR}^{-1/2}[\mathbf{z} \mathbf{Z}]$ is independent of \mathbf{R} under H_0 . Iterating this reasoning it is also straightforward to show that the joint distribution of $\widehat{\gamma}^{1,(t+1)}, \widehat{\gamma}^{1,(t)}$ and the entries of $\mathbf{UR}^{-1/2}[\mathbf{z} \mathbf{Z}]$ and eventually that of $\widehat{\gamma}^{1,(t+1)}, \widehat{\gamma}^{1,(t)}, \widehat{\gamma}^{0,(t+1)}, \widehat{\gamma}^{0,(t)}$ and the entries of $\mathbf{UR}^{-1/2}[\mathbf{z} \mathbf{Z}]$ is independent of \mathbf{R} .

Proof of Theorem 1

Iterative application of Lemma 1, starting with the assumption that the joint distribution of the RVs $\widehat{\gamma}_k^{1,(0)}, \widehat{\gamma}_k^{0,(0)}, k = 1, \dots, K$, and the entries of $\mathbf{UR}^{-1/2}[\mathbf{z} \mathbf{Z}]$ is independent of \mathbf{R} , leads to a joint distribution of the RVs $\widehat{\gamma}^{1,(t_{\max})}, \widehat{\gamma}^{1,(t_{\max}-1)}, \widehat{\gamma}^{0,(t_{\max})}, \widehat{\gamma}^{0,(t_{\max}-1)}$ and the entries of $\mathbf{UR}^{-1/2}[\mathbf{z} \mathbf{Z}]$ independent of \mathbf{R} . It follows that the statistic of the proposed detector, given by eq. (10), can be written as

$$\frac{\left[\frac{\prod_{k=1}^K \widehat{\gamma}_k^{0,(t_{\max})}}{\prod_{k=1}^K \widehat{\gamma}_k^{1,(t_{\max})}} \right]^{\frac{N}{K+1}} \det \left[\mathbf{U}\boldsymbol{\zeta}\boldsymbol{\zeta}^\dagger \mathbf{U}^\dagger + \sum_{k=1}^K \frac{\mathbf{U}\boldsymbol{\zeta}_k \boldsymbol{\zeta}_k^\dagger \mathbf{U}^\dagger}{\widehat{\gamma}_k^{0,(t_{\max})}} \right]}{\det \left[\left(\mathbf{U}\boldsymbol{\zeta} - \frac{(\mathbf{c}^{(t_{\max}-1)})^\dagger \mathbf{U}\boldsymbol{\zeta}}{(\mathbf{c}^{(t_{\max}-1)})^\dagger \mathbf{e}_1} \mathbf{e}_1 \right) \left(\mathbf{U}\boldsymbol{\zeta} - \frac{(\mathbf{c}^{(t_{\max}-1)})^\dagger \mathbf{U}\boldsymbol{\zeta}}{(\mathbf{c}^{(t_{\max}-1)})^\dagger \mathbf{e}_1} \mathbf{e}_1 \right)^\dagger + \sum_{k=1}^K \frac{\mathbf{U}\boldsymbol{\zeta}_k \boldsymbol{\zeta}_k^\dagger \mathbf{U}^\dagger}{\widehat{\gamma}_k^{1,(t_{\max})}} \right]},$$

where $(\mathbf{c}^{(t_{\max}-1)})^\dagger$, defined after eq. (A.13) in the proof of Lemma 1, is a function of $\widehat{\gamma}^{1,(t_{\max}-1)}$ and the entries of $\mathbf{UR}^{-1/2} \mathbf{Z}$ and hence, the theorem is proved.

Proof of Lemma 2

First observe that $\widehat{\alpha}^{(t+1)}$, given by eq. (5), is independent of $\gamma_1, \dots, \gamma_K$ and can be expressed in terms of \mathbf{z} and \mathbf{G} . Moreover, $\mathbf{B}_h^{1,(t+1)}$, given by eq. (6), is independent of $\gamma_1, \dots, \gamma_K$ and can be expressed in terms of \mathbf{z} and \mathbf{G} .

Thus $\hat{\gamma}_k^{1,(t+1)}$, given by eq. (7), can be expressed as $\hat{\gamma}_k^{1,(t+1)} = \gamma_k g_k^{1,(t+1)}(\mathbf{z}, \mathbf{G})$ and the lemma is proved.

Proof of Theorem 2

Iterative application of Lemma 2, starting with the assumption that $\hat{\gamma}_k^{1,(0)} = \gamma_k g_k^{1,(0)}(\mathbf{z}, \mathbf{G})$ and $\hat{\gamma}_k^{0,(0)} = \gamma_k g_k^{0,(0)}(\mathbf{z}, \mathbf{G})$, $k = 1, \dots, K$, is independent of $\gamma_1, \dots, \gamma_K$, leads to $\hat{\gamma}_k^{1,(t_{\max})} = \gamma_k g_k^{1,(t_{\max})}(\mathbf{z}, \mathbf{G})$ and $\hat{\gamma}_k^{0,(t_{\max})} = \gamma_k g_k^{0,(t_{\max})}(\mathbf{z}, \mathbf{G})$, $k = 1, \dots, K$. Then, it is sufficient to observe that $\hat{\alpha}^{(t_{\max})}$, given by eq. (A.12), is independent of $\gamma_1, \dots, \gamma_K$ and can be expressed in terms of \mathbf{z} , $g_1^{1,(t_{\max}-1)}(\mathbf{z}, \mathbf{G}), \dots, g_K^{1,(t_{\max}-1)}(\mathbf{z}, \mathbf{G})$. We can conclude that the statistic of the proposed detector, given by eq. (10), is independent of $\gamma_1, \dots, \gamma_K$ (under H_0).

References

- [1] W. Melvin, J. Scheer, Principles of Modern Radar: Radar Applications, Vol. 3 of Electromagnetics and Radar, Institution of Engineering and Technology, 2013.
- [2] E. J. Kelly, An adaptive detection algorithm, IEEE Trans. Aerosp. Electron. Syst. (2) (1986) 115–127.
- [3] F. C. Robey, D. R. Fuhrmann, E. J. Kelly, R. Nitzberg, A CFAR adaptive matched filter detector, IEEE Trans. Aerosp. Electron. Syst. 28 (1) (1992) 208–216.
- [4] F. Bandiera, D. Orlando, G. Ricci, Advanced Radar Detection Schemes Under Mismatched Signal Models, San Rafael, US, 2009.

- [5] W. Liu, J. Liu, C. Hao, Y. Gao, Y. Wang, Multichannel adaptive signal detection: Basic theory and literature review, 2021.
- [6] K. D. Ward, Compound representation of high resolution sea clutter, *Elect. Lett.* 17 (16) (6th August 1981) 561–563.
- [7] K. D. Ward, C. J. Baker, S. Watts, Maritime surveillance radar. part 1: Radar scattering from the ocean surface, *Inst. Elect. Eng. Proc. F* 137 (2) (1990) 51–62.
- [8] A. Farina, F. Gini, M. V. Greco, L. Verrazzani, High resolution sea clutter data: statistical analysis of recorded live data, *IEE Proc. - Radar, Sonar and Navig.* 144 (3) (1997) 121–130.
- [9] M. Greco, F. Gini, M. Rangaswamy, Statistical analysis of measured polarimetric clutter data at different range resolutions, *IEE Proc.-Radar Sonar Navig.* 153 (6) (2006) 473–481.
- [10] K. D. Ward, R. J. A. Tough, S. Watts, *Sea Clutter, Scattering, the K distribution and radar performance*, 2nd Edition, Inst of Engineering & Technology, 2013.
- [11] E. Conte, M. Longo, Characterisation of radar clutter as a spherically invariant random process, *IEE Proc. F - Commun., Radar and Sig. Process.* 134 (2) (1987) 191–197.
- [12] E. Conte, M. Longo, M. Lops, Modelling and simulation of non-rayleigh radar clutter, *IEE Proc. F - Radar and Sig. Process.* 138 (2) (1991) 121–130.

- [13] E. Conte, M. Lops, G. Ricci, Asymptotically optimum radar detection in compound-gaussian clutter, *IEEE Trans. Aerosp. Electron. Syst.* 31 (2) (1995) 617–625.
- [14] S. Kraut, L. L. Scharf, The CFAR adaptive subspace detector is a scale-invariant GLRT, *IEEE Trans. Signal Process.* 47 (9) (1999) 2538–2541.
- [15] J. Liu, D. Massaro, D. Orlando, A. Farina, Radar Adaptive Detection Architectures for Heterogeneous Environments, *IEEE Trans. Signal Process.* 68 (2020) 4307–4319.
- [16] M. J. Steiner, K. Gerlach, Fast converging adaptive processor on a structured covariance matrix, *IEEE Trans. Aerosp. Electron. Syst.* 36 (4) (2000) 1115–1126.
- [17] Y. I. Abramovich, N. K. Spencer, G. A. Y., Modified GLRT and AMF Framework for Adaptive Detectors, *IEEE Trans. Aerosp. Electron. Syst.* 43 (3) (2007) 1017–1051.
- [18] E. Ollila, D. E. Tyler, Regularized M -Estimators of Scatter Matrix, *IEEE Transactions on Signal Processing* 62 (22) (2014) 6059–6070.
- [19] A. Coluccia, Regularized Covariance Matrix Estimation Via Empirical Bayes, *IEEE Signal Processing Letters* 22 (11) (2015) 2127–2131.
- [20] D. Xu, P. Addabbo, C. Hao, J. Liu, D. Orlando, A. Farina, Adaptive strategies for clutter edge detection in radar, *Signal Processing* 186 (2021) 108127.

- [21] P. Addabbo, S. Han, D. Orlando, G. Ricci, Learning Strategies for Radar Clutter Classification, *IEEE Trans. Signal Process.* 69 (2021) 1070–1082.
- [22] S. Han, P. Addabbo, D. Orlando, G. Ricci, Radar Clutter Classification Using Expectation-Maximization Method, in: *ICASSP 2021 - 2021 IEEE International Conference on Acoustics, Speech and Signal Processing (ICASSP)*, 2021, pp. 4585–4589.
- [23] M. C. Wicks, W. L. Melvin, P. Chen, An efficient architecture for non-homogeneity detection in space-time adaptive processing airborne early warning radar, in: *Radar 97 (Conf. Publ. No. 449)*, 1997, pp. 295–299.
- [24] R. S. Adve, T. B. Hale, M. C. Wicks, Transform domain localized processing using measured steering vectors and non-homogeneity detection, in: *Proceedings of the 1999 IEEE Radar Conference. Radar into the Next Millennium (Cat. No.99CH36249)*, 1999, pp. 285–290.
- [25] M. Rangaswamy, Statistical analysis of the nonhomogeneity detector for non-Gaussian interference backgrounds, *IEEE Trans. Signal Process.* 53 (6) (2005) 2101–2111.
- [26] E. Conte, A. De Maio, G. Ricci, Covariance matrix estimation for adaptive CFAR detection in compound-gaussian clutter, *IEEE Trans. Aerosp. Electron. Syst.* 38 (2) (2002) 415–426.
- [27] E. Conte, A. De Maio, G. Ricci, Recursive estimation of the covariance matrix of a compound-gaussian process and its application to adaptive CFAR detection, *IEEE Trans. Signal Process.* 50 (8) (2002) 1908–1915.

- [28] M. S. Greco, F. Gini, Covariance matrix estimation for CFAR detection in correlated heavy tailed clutter, *Signal Process.* 82 (12) (2002) 1847–1859.
- [29] E. Conte, A. De Maio, Mitigation techniques for non-gaussian sea clutter, *IEEE Journal of Oceanic Engineering* 29 (2) (2004) 284–302.
- [30] F. Pascal, Y. Chitour, J. Ovarlez, P. Forster, P. Larzabal, Covariance structure maximum-likelihood estimates in compound gaussian noise: Existence and algorithm analysis, *IEEE Trans. Signal Process.* 56 (1) (2008) 34–48.
- [31] P. Stoica, Y. Selen, Cyclic minimizers, majorization techniques, and the expectation-maximization algorithm: a refresher, *IEEE Signal Processing Magazine* 21 (1) (2004) 112–114.
- [32] E. Conte, M. Lops, G. Ricci, Adaptive Radar Detection in Compound-Gaussian Clutter, in: *Seventh European Signal Processing Conference (EUSIPCO-94)*, Edinburgh, Scotland (UK), 1994.
- [33] H. Lütkepohl, *Handbook of Matrices*, John Wiley & Sons, 1996.
- [34] J. B. Billingsley, A. Farina, F. Gini, M. S. Greco, L. Verrazzani, Statistical Analyses of Measured Radar Ground Clutter Data, *IEEE Transactions on Aerospace and Electronic Systems* 35 (2) (1999) 579–593.
- [35] M. Greco, F. Gini, A. Farina, J. B. Billingsley, Validation of windblown radar ground clutter spectral shape, *IEEE Transactions on Aerospace and Electronic Systems* 37 (2) (2001) 538–548.